J Therm Anal Calorim (2012) 108:627–631
DOI 10.1007/s10973-011-1944-4

# Triple point measurements for alternative refrigerants

**Giovanni Di Nicola · Caterina Brandoni ·
Cristiano Di Nicola · Giuliano Giuliani**

MEDICTA2011 Conference Special Chapter

**Abstract** Triple point data are important in the refrigerating industry, defining the lowest temperature limit at which a refrigerant may circulate in a fluid state. For several refrigerants, triple point data present in the literature are extremely scarce or inaccurate. A recently developed Solid–Liquid Equilibria (SLE) apparatus was used to measure the triple point temperature of 16 of the most widely applied alternative refrigerants, namely three methane derivatives (fluoromethane, R41; difluoromethane, R32; trifluoromethane, R23), four ethane derivatives (pentafluoroethane, R125; 1,1,1,2-tetrafluoroethane, R134a; 1,1,1-trifluoroethane, R143a; 1,1-difluoroethane, R152a), five propane derivatives [1,1,1,2,3,3,3-heptafluoropropane, R227ea; 1,1,2,3,3,3-hexafluoropropane, R236ea; 1,1,1,3,3-Pentafluoropropane, R245fa; 1,1,2,2,3-pentafluoropropane, R245ca; 1,1,1,3,3,3-hexafluoropropane, R236fa), and four hydrofluoro-olefines (2,3,3,3-tetrafluoroprop-1-ene, R1234yf; trans-1,3,3,3 tetrafluoropropene, R1234ze(E); 3,3,3-trifluoropropene, R1243zf; 1,2,3,3,3-pentafluoropropene, 1225 ye(Z)]. The experimental setup, that was recently adopted for the SLE estimation of binary systems containing carbon dioxide (J Therm Anal Calorim 105:489–493, 2011), comprises a measuring cell and a system for drawing the liquid nitrogen directly from its insulated tank with the aid of compressed air: the carrier fluid circulating in the circuit is thus the refrigerant itself. The measurements were performed both in the heating and in the cooling mode. In order to confirm the functional efficiency and fine adjustment of the apparatus, the already available triple point literature data for carbon dioxide, dimethyl ether, and nitrous oxide were also compared with the ones measured by the present setup, confirming the validity of the setup. The measured triple point data for the refrigerants revealed generally good agreement with the literature, excepting a few fluids that revealed some discrepancies.

**Keywords** Experimental · Refrigerants · Temperature · Triple point

## Experimental setup and procedure

The apparatus comprises a measuring cell and a system for drawing the liquid nitrogen directly from its insulated tank with the aid of compressed air: the carrier fluid circulating in the circuit is thus the refrigerant itself.

The experimental setup is shown in Fig. 1. The measuring cell (1) was made out of a stainless steel cylinder with a cover welded to the body. The volume was approximately 47 $cm^3$.

A stirrer (2) was placed in the cell. Two holes were drilled in the cover, and a stainless steel tube with a diameter of 4 mm was inserted through and welded to the hole on the left for charging the cell with gas, while the hole on the right was used to house the thermometer with a diameter of 3 mm (3). The purpose of the stirrer was to prevent any premature stratification of the fluids comprising the various mixtures, while also assuring greater homogeneity during the liquefaction and crystallization of the mixture. The stirrer inside the cell was turned by a

G. Di Nicola (✉) · C. Di Nicola · G. Giuliani
DIISM, Università Politecnica delle Marche,
Via Brecce Bianche, 60100 Ancona, Italy
e-mail: g.dinicola@univpm.it

C. Brandoni
Università degli Studi e-Campus, Via Isimbardi 10,
22060 Novedrate, CO, Italy

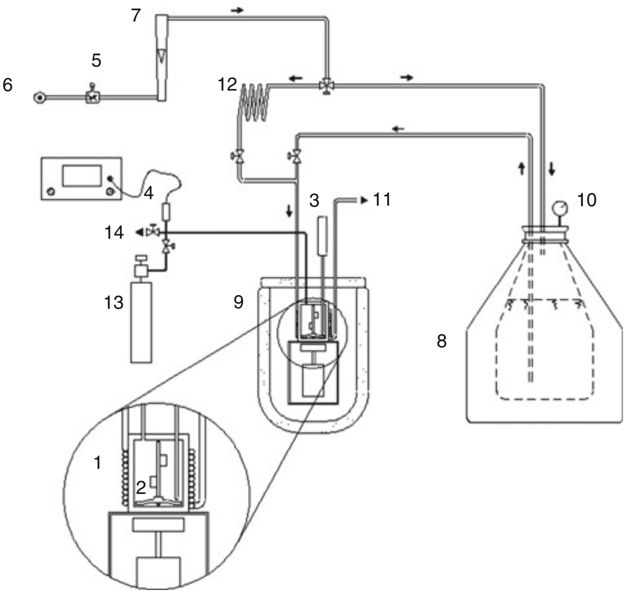

**Fig. 1** Schematic illustration of the apparatus. Notation: *1* measurement cell, *2* stirrer, *3* platinum resistance thermometer, *4* pressure transducer, *5* mass flow controller, *6* dry air supplier, *7* rotameter, *8* liquid nitrogen tank, *9* dewar containing the measurement cell, *10* liquid nitrogen dewar manometer, *11* nitrogen outlet, *12* external heating coil, *13* charging bottle, *14* vacuum pump system

magnet, which drives the plate welded onto the lower end of the rod.

An absolute pressure transducer (HBM, Mod. P8A) (4) was installed in the charging tube. A mass flow controller (5) was installed upstream from the dehumidifier: a needle valve with a shutter was used to adjust the flow rate coming from the dry air supplier (6), as measured by means of the pressure difference read on a pressure gauge alongside it. The airflow was also measured by a rotameter (7).

The operation of the system as a whole can be divided into two separate circuits and consequently two operating modes: a cooling and a heating mode.

### Cooling mode

The cooling system as a whole is composed of four functional parts: the compressed air circuit that creates a positive pressure in the liquid nitrogen tank, the thermally insulated liquid nitrogen tank (8), the hose connecting the tank to the circuit, complete with a faucet, and the copper coil that surrounds and exchanges heat with the cell.

The core element in the whole cooling system is the copper coil surrounding the measuring cell; through its contact surface, the coil removes heat by means of the refrigerant fluid flowing inside it. The copper coil and cell are placed together inside a Dewar flask (9) so as to further isolate them from the outside environment. The system as a whole is suitably covered with neoprene foam for thermal insulation.

When the system is used in the cooling mode, the compressed air (after passing through suitable dehumidifier filters) is delivered to the liquid nitrogen tank, which is thus placed under positive pressure. Inside the tank, a poly(vinyl chloride) (PVC) hose draws the refrigerant fluid from the bottom, which begins to flow through the circuit as soon as the pressure in the tank, controlled by a manometer (10), is sufficient to overcome the load losses produced by the circuit. When a steady state is reached, the liquid nitrogen flows through the circuit, rapidly cooling all of its surfaces down to temperatures of about 100 K. The refrigerant fluid passes first through the silicone capillary, then through the copper piping, exchanging heat with the measuring cell by evaporation as it moves through the coil, and finally flows out from the nitrogen outlet (11). In this cooling configuration, the nitrogen valve remains open, and the heating circuit valve remains closed.

### Heating mode

When the system is operated in the heating mode, the dehumidified compressed air circuit is connected directly to the measuring cell's circuit, and in this case, the air acts as a carrier fluid and warms the cell, which is at temperatures of about 100 K at the end of the measuring procedure. In this configuration, the nitrogen inlet valve remains closed. An external copper coil (12) has also been provided: this can be heated by the operator to speed up the warming of the measuring cell.

### Temperature

To monitor the temperatures, the apparatus was equipped with one thermoresistor placed in the measuring cell. In order to measure the temperature exactly in the middle and along the boundary of the cell having a smaller sensor, the thermoresistor was replaced with two thermocouples. Data were recorded with both experimental devices.

The platinum resistance thermometer (model: S7929, 100 Ω, Minco) and the thermocouples used in the apparatus were calibrated by comparison with a 25 Ω platinum resistance thermometer (model: 5680, SN1083, Hart Scientific) already presented elsewhere [1].

### Experimental procedure

The charging procedure consisted of the bottle containing the refrigerant gas (13) was weighed on an electronic balance (the uncertainty of which is 0.5 mg). Then, the bottle was connected to the apparatus and to the vacuum pump (14) (Vacuubrand, mod. RZ2), and a vacuum was created inside the measuring cell and the charging tube as recorded on the vacuum pump gauge (Galileo, mod. OG510). Then, the fluid was charged by opening the valve on the gas bottle; the temperature of the cell was brought down by a flow of liquid nitrogen so as to insert the whole mass in the cell, leaving as little as possible in the charging tube. A suitable time interval was allowed so that the pressure, being lowered by the temperature reduction, could drop to below atmospheric pressure, and then the on/off valve was closed; the gas bottle was disconnected and weighed again to establish the actual mass charged in the cell.

The coil with liquid nitrogen was wrapped around the measuring cell. By monitoring the time dependence of temperature, a cooling curve was obtained. While the change of phase occurs, the heat removed by cooling is compensated for by the latent heat of the phase change, showing a change of slope in the temperature trend.

The arrest in cooling during the solidification allows the melting point of the material to be identified on the time–temperature curve.

### Experimental uncertainties

All of the uncertainties were calculated using the law of error propagation, as reported elsewhere [2]. Here, the previously reported results will be briefly summarized. The global uncertainty of the temperature, considering also the contribution of the Rossini method correction, was estimated to be less than ±0.8 K, both for thermoresistor and thermocouple measurements.

Since the measured vapor pressure data were not accurately measured at very low temperatures within the declared precision of the used instrument (the pressure values were acquired by an absolute pressure transducer HBM, model: P8A, and the global uncertainty of the pressure measurements was estimated to be less than 3 kPa), the vapor pressure data are not reported in the present paper.

## Experimental results

In order to confirm the functional efficiency and fine adjustment of the apparatus, the already available triple point literature data for two inorganic compounds (carbon dioxide and nitrous oxide) and dimethyl ether were compared with the ones measured by the present setup, both by using a thermoresistor and the thermocouples.

In Table 1, the summary of all the experimental measurements are reported together with data from the open literature ($T_{\mathrm{lit}}$). The table reports the average of the triple point measurements obtained by the thermoresistor in the cooling mode ($T_{1,\mathrm{c}}$), and by the thermocouple in the cooling ($T_{2,\mathrm{c}}$) and in the heating mode ($T_{2,\mathrm{h}}$).

The triple point measurements obtained by the thermoresistor in the heating mode are not reported because the change of phase was not clearly evident. In addition, the measurements obtained by the thermocouples in the center and in the boundary of the cell gave generally the same results and here, only the values measured in the center of the cell are reported. Figure 2 shows an example of acquisition for R236fa obtained in the heating mode and with the thermocouples placed both in the middle and in the boundary of the cell.

As a first part of the experimental acquisitions, measurements were performed for several fluids (inorganic fluids, methane and ethane derivatives) adopting a thermoresistor. More recently, the measurements were repeated for all the fluids (including also the propane derivatives) adopting two thermocouples placed in the center and in the boundary of the cell. The thermoresistor measurements generally showed slightly better agreement with the literature values; however, also the thermocouples gave good results, both for the heating and the cooling mode. In addition, no relevant difference (well within the experimental uncertainty) was found from the measurements in the middle and along the boundary of the cell.

For inorganic compounds, also due to the higher triple point temperatures, results were found to be in a very good agreement (few tenths of a Kelvin) with the literature sources. The average of the measurements obtained for the methane derivatives showed very good agreement for R41 and some discrepancy for R23 and R32. Good agreement was also found for ethane derivatives. The average of the measurements obtained for the five propane derivatives were compared with the unique literature source [3]. Good agreement (within ±1 K) was found for R227ea, R236ea, R236fa, and R245fa, while a higher discrepancy was found for R245ca, probably due to the difference in sample purity (99.9% against 99.5%).

The average of the measurements obtained for the two propene derivatives for which literature data are available [R1234yf and R1234ze(E)], showed a very good agreement with the sources, especially for the results obtained from the thermocouples (R1234yf) and by the cooling mode (R1234ze(E)). For R1243zf and 1225ye(Z), the change of phase was evident only in the cooling mode and for the thermocouple measurements. For both fluids, no data are available in the open literature.

The results of the temperature data acquisitions were corrected using the Rossini method [4] because a constant cooling rate is not needed and was not guaranteed by our experimental method. This is a graphic method that considers the area contained by the tangent to the curve in the descending stretch after the temperature drop, and curve

**Table 1** Triple point values

| Fluid | Sample purity/% | $T_{li}$/K | Source | $T_{1,c}$/K | $T_{2,c}$/K | $T_{2,h}$/K |
|---|---|---|---|---|---|---|
| $CO_2$ | 99.99 | 216.58 | [5] | 216.6 | 216.5 | 216.3 |
| $N_2O$ | 99.99 | 182.34 | [6, 7] | 182.0 | 181.7 | 182.0 |
| DME | 99.8 | 131.65 | [8, 9] | 131.6 | 131.6 | 131.6 |
| R23 | 99.6 | 118.02 | [10] | 117.7 | 117.0 | 116.6 |
| R32 | 99.98 | 136.34 | [11] | 137.1 | 135.7 | 135.3 |
| R41 | 99.9 | 129.82 | [12] | 129.8 | 129.8 | 129.8 |
| R125 | 99.96 | 172.52 | [11] | 173.0 | 172.5 | 172.5 |
| R134a | 99.98 | 169.85 | [13] | 169.7 | 169.8 | 169.8 |
| R143a | 99.9 | 161.34 | [14] | 161.4 | 161.4 | 161.6 |
| R152a | 99.94 | 154.30 | [14, 15] | 154.3 | 154.3 | 154.3 |
| R227ea | 99.7 | 146.35 | [3] | – | 145.9 | 144.7 |
| R236ea | 99.99 | 127.05 | [3] | – | 126.6 | 126.8 |
| R236fa | 99.94 | 178.95 | [3] | – | 179.8 | 179.6 |
| R245ca | 99.9 | 199.75 | [3] | – | 196.0 | 195.7 |
| R245fa | 99.97 | 171.05 | [3] | – | 170.0 | 170.2 |
| R1234yf | 99.9 | 122.77 | [16] | 123.45 | 122.6 | 122.6 |
| R1234ze(E) | 99.9 | 168.62 | [17] | – | 168.8 | 169.3 |
| R1243zf | 99.9 | – | – | – | 122.8 | – |
| R1225ye(Z) | 99.9 | – | – | – | 134.3 | – |

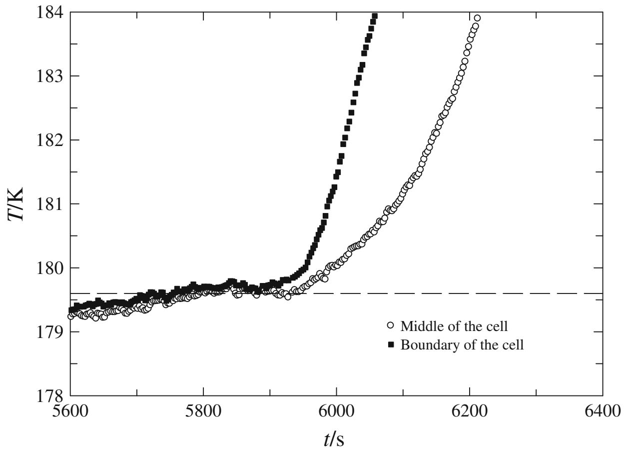

**Fig. 2** An example for R236fa obtained in the heating mode

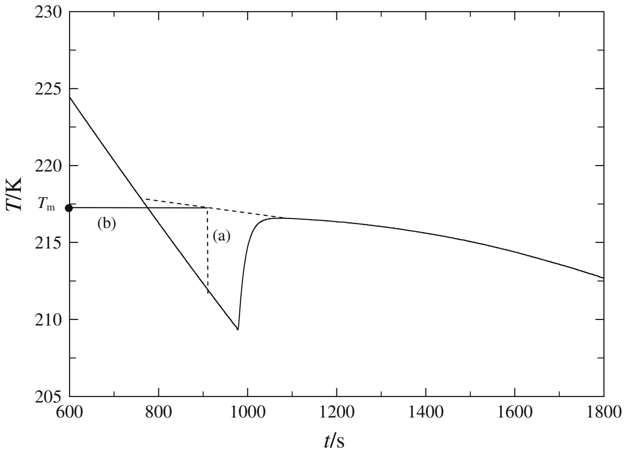

**Fig. 3** Representation of the Rossini method [4] for triple point measurement of $CO_2$ and acquisition in the cooling mode example

itself; then a vertical segment (a) is taken, which divides the area into two equal parts; then a second, horizontal segment (b) is obtained, from the point of intersection between the segment (a) and the tangent to the curve, up until it identifies the temperature corresponding to this new point on the axis of the ordinates ($T_m$). This graphical method, together with an acquisition obtained for carbon dioxide in the cooling mode, is illustrated in Fig. 3.

The amount of the corrections takes into account the fact that the fluid is still in a liquid state during the metastable state (supercooling) prior to solidification. In this phase, the temperature is distinctly lower than the one characterizing the instant when crystallization begins, its amplitude depending mainly on the rate at which the temperature is lowered. The resulting corrections were nonetheless always very limited, of the order of a few tenths of a Kelvin in the majority of cases, and always well below the estimated uncertainty.

## Conclusions

The triple point of several refrigerants was measured with an experimental setup that was formerly used for the study of the SLE of binary systems containing carbon dioxide [18].

The experimental method was validated by measuring the triple points of well known inorganic fluids (carbon dioxide and nitrous oxide) and dimethyl ether. Different measurement mode were tested, delivering slightly different results; however, both within the experimental uncertainties.

## References

1. Arteconi A, Di Nicola G, Moglie M, Santori G, Stryjek R. Alternative biofuels: *PVT*x measurements for DME + propane. J Therm Anal Calorim. 2010;99:899–903.
2. Di Nicola G, Giuliani G, Polonara F, Stryjek R. Solid-liquid equilibria for the $CO_2$ + R125, and $N_2O$ + R125 systems: a new apparatus. J Chem Eng Data. 2006;51:2209–14.
3. Beyerlein AL, DesMarteau DD, Hwang SH, Smith ND, Joyner PA. Physical properties of fluorinated propane and butane derivatives as alternative refrigerants. ASHRAE Trans. 1993;99: 368–79.
4. Mair BJ, Glasgow JAR, Rossini FD. Determination of the freezing points and amounts of impurity in hydrocarbons from freezing and melting curves. J Res Nat Bur Standards. 1941;26: 591–620.
5. Angus S, Armstrong B, de Reuck KM. International thermodynamic tables of the fluid state—3 carbon dioxide. New York: Pergamon; 1976.
6. Calado JCG, Rebelo LPN, Streett WB, Zollweg JA. Thermodynamics of liquid (dimethylether + xenon). J Chem Thermodyn. 1986;18:931–8.
7. Fonseca IMA, Lobo LQ. Thermodynamics of liquid mixtures of xenon and methyl fluoride. Fluid Phase Equilib. 1989;47:249–63.
8. Ihmels EC, Lemmon EW. Experimental densities, vapor pressures, and critical point, and a fundamental equation of state for dimethyl ether. Fluid Phase Equilib. 2007;260:36–48.
9. Stull DR, EF Westrum Jr, Sinke GC. The chemical thermodynamics of organic compounds. New York: John Wiley and Sons; 1969.
10. Magee JW, Duarte-Garza HA. Molar heat capacity at constant volume of trifluoromethane (R23) from the triple-point temperature to 342 K at pressures to 33 MPa. Int J Thermophys. 2000;21:1351–72.
11. Lüddecke TO, Magee JW. Molar heat capacity at constant volume of difluoromethane (R32) and pentafluoroethane (R125) from the triple-point temperature to 345 K at pressures to 35 MPa. Int J Thermophys. 1996;17:823–49.
12. Magee JW. In: Holcomb CD, Magee JW, Scott JL, Outcalt SL, Haynes WM, editors. NIST technical note 1397; 1997. p. 14.
13. Tillner-Roth R, Baehr HD. An international standard formulation of the thermodynamic properties of 1, 1, 1, 2-tetrafluoroethane (HFC-134a) for temperatures from 170 K to 455 K at pressures up to 70 MPa. J Phys Chem Ref Data. 1994;23:657–729.
14. Magee JW. Molar heat capacity at constant volume of 1,1-difluoroethane (R152a) and 1,1,1-trifluoroethane (R143a) from the triple-point temperature to 345 K at pressures to 35 MPa. Int J Thermophys. 1998;19:1397–420.
15. Blanke W, Weiss R. Isochoric (p, v, T) measurements on C2H4F2 (R152a) in the liquid state from the triple point to 450 K and at pressures up to 30 MPa. Fluid Phase Equilib. 1992;80: 179–90.
16. Minor B, Spatz M. HFO-1234yf low GWP refrigerant update. International refrigeration and air conditioning conference at Purdue, paper 2349, 14–17 July 2008, pp. 1–8.
17. Lemmon EW, Huber ML, McLinden MO. NIST standard reference database 23: reference fluid thermodynamic and transport properties-REFPROP, Version 9.0, National Institute of Standards and Technology, Standard Reference Data Program, Gaithersburg; 2010.
18. Di Nicola G, Moglie M, Stryjek R, Santori G. Solid–liquid equilibria for the dimethyl ether + carbon dioxide binary system. J Therm Anal Calorim. 2011;105:489–93.